

# Edge Detection Using Wavelet Scale Correlation



By

Lt Col Asad Anwar

Submitted to the Faculty of Electrical Engineering  
National University of Sciences and Technology, Rawalpindi in partial  
fulfillment for the requirements of a M.S Degree in Telecomm

MAR 2012

# *Acknowledgements*

*My first, and most earnest, acknowledgment goes to my supervisor Lt Col Dr. Imran Touqir for his guidance, encouragement, help throughout my course work and research and being patient while I could not divert my attention to my work due to my service obligations during off campus time. I am grateful to faculty of Electrical Engineering for teaching the core courses. I am thankful to my committee members Col Attiq Ahmed, faculty member EE Dept, Maj Dr Asif Masood, faculty member CS Dept and Maj Dr Adil Masood Saddique, faculty member EE Dept, for their assistance and valuable guidance in accomplishing my work. I do acknowledge the support in terms of distance learning multimedia lectures (thanks to Dr. Imran Touqir and Maj Dr Adil Masood Saddique to provide me such valuable material on the subject) on wavelets of Prof Gilbert Strang, MIT and Dr. Imtiaz Taj, CARE, Islamabad.*

*I want to thank my friends and colleagues who have spent time in providing me assistance in software development, especially Iftikhar Qureshi for whom I have great regard, and I wish to extend my warmest thanks to him.*

*I owe my most sincere gratitude to Pakistan Army for sponsoring my education after high school till to date. I do acknowledge the conducive environment provided by Military College of Signals for quality education.*

*My final, and most heartfelt, acknowledgment must goes to my mother and my wife for taking all the social and administrative responsibilities of home and the*

*children and providing me the opportunity to undergo the research work with zeal.*

# Abstract

The spatial domain, frequency domain and wavelet based techniques are being used independently to detect edges in an image. Spatial filters are very good at localization accuracy but do not have any control over the operator's scale. Similarly Fourier transform being global in nature can neither localize sharp transients nor differentiate between true and false edges. The problem aggravates further under noisy scenario. The classical edge detectors do not yield adequate edge maps of the noisy images and malfunction over default threshold values. The choice of optimum threshold for edge detection is not generic for diverse set of images and noise models. A good threshold assigned to yield a good edge map for a particular type of image and noise model may be inappropriate for other type of image or the different noise model/intensity in the image. Thus it requires user's intervention to assign suitable threshold value to differentiate between true and false edges. Thus the two major dilemmas for edge detection are firstly the choice of appropriate threshold to segregate noise and true edges and secondly to opt for an appropriate scale for edge detection.

In this research work a novel edge detection paradigm is envisaged to work for various images. The image is decomposed by multilevel wavelet decomposition using Quadrature mirror filters and then thresholded. The decomposition level is determined by the image resolution. The property that image structural details remain present at each level whereas noise is partially eliminated within subbands, is being exploited. The lower resolution wavelet detail bands are interpolated to the original image size which partially recaptures the missing edge pixels besides facilitating matrix multiplications. An innovative wavelet synthesis approach is conceived based on wavelet scale correlation of the concordant detail bands such that the reconstructed image fabricates an edge map of the image.

# Table of Contents

Acknowledgements	li
Abstract	lii
List of Figures	Vi
List of Acronyms	Ix
1 Introduction	1
1.1 Existing Techniques on Edge Detection	2
1.1.1 Spatial Operators	3
1.1.2 Frequency Domain Filters	4
1.1.3 Multi-Resolution Analysis	5
1.2 Noise Models	5
1.3 Objectives	6
1.4 Author's Contribution	7
1.5 Thesis Organization	8
2 Classical Edge Detectors	9
2.1 Edge Detection	9
2.2 Spatial Domain Filters	10
2.2.1 Gradient Operators	11
2.2.1.1 Sobel Gradient Operator	13
2.2.1.2 Prewitt Gradient Operator	13
2.2.1.3 Robert's Cross Operator	13
2.2.2 Second Derivative Operators	14
2.2.2.1 Laplacian Operator	14
2.2.2.2 The Marr–Hildreth operator	16
2.2.3 Canny's Edge Detection Algorithm	17
2.2.4 Implementation of Classical Operators	21
2.2.5 Performance of Edge Detection Algorithms	24
2.3 Frequency Domain Filters	25
2.4 Effects of Noise on Edge Detection	27
2.4.1 Noise models	27
2.4.1.1 Gaussian Noise	28
2.4.1.2 Rayleigh noise	29
2.4.1.3 Exponential noise	30
2.4.1.4 Uniform Noise	30
2.4.1.5 Impulse (Salt-and-Pepper) Noise	31
2.4.2 Implementation of Classical Operators under Noisy Scenario	33

2.5 Conclusion	38
3 Wavelets and Edge Detection	40
3.1 Historical Perspective	40
3.2 Short Time Fourier Transform	42
3.3 Continuous Wavelet Transform (CWT)	44
3.4 Wavelet Properties	45
3.5 Discrete Wavelets	47
3.6 A Band-Pass Filter	50
3.7 The Scaling Function	51
3.8 Subband Coding	53
3.9 The Discrete Wavelet Transform	56
3.10 Edge Detection	60
3.11 Conclusion	61
4 Novel Edge Detector	62
4.1 Edge Thinning	63
4.1.1 Thinning Rules	63
4.2 Novel Wavelet Synthesis for Edge Detection	65
4.3 Graphical User Interface for Software Development	71
4.4 Experimental Results	71
4.4 Conclusion	74
4.5 Future Work	75
Appendix A: Standard Bench mark Images used in Thesis	76
Appendix B: Snapshots of GUI used in development of software	77
References	79

vi

## List of Figures

<b>Figure 2.1</b> Edge Detection through First and Second Derivative operators	11
<b>Figure 2.2</b> Horizontal and Vertical 3 x3 Convolution masks	12
<b>Figure 2.3</b> Sobel Kernels	13
<b>Figure 2.4</b> Prewitt Kernels	13
<b>Figure 2.5</b> Robert's cross Kernels	14
<b>Figure 2.6</b> Laplacian Template	15
<b>Figure 2.7</b> Laplacian of Gaussian operator and its discrete approximation	17
<b>Figure 2.8</b> 5x5 image	20
<b>Figure 2.9</b> Edge Directions	20
<b>Figure 2.10</b> Edges detected from Lena image by conventional operators	22
<b>Figure 2.11</b> Edges detected from Building image by conventional operators	22

<b>Figure 2.12</b>	Edges detected from Boat image by conventional operators	23
<b>Figure 2.13</b>	Edges detected from House image by conventional operators	23
<b>Figure 2.14</b>	Edges detected from Camera Man image by conventional Operators	24
<b>Figure 2.15</b>	Edge detection in frequency domain	26
<b>Figure 2.16</b>	Edges detected by highpass filtering from bench images (a) Lena (b)House (c) Cameraman	27
<b>Figure 2.17</b>	Probability Distribution Function of Gaussian Noise	28
<b>Figure 2.18</b>	Probability Distribution Function of Rayleigh Noise	29
<b>Figure 2.19</b>	Probability Density Function of Exponential Noise	30
<b>Figure 2.20</b>	Probability Density Function of Uniform Noise	31
<b>Figure 2.21</b>	Density Function of Impulse Noise	32
<b>Figure 2.22</b>	Edges from Lina image with Gaussian Noise $N(0, 0.01)$ by classical operators	33
<b>Figure 2.23</b>	Edges from Building image with Gaussian Noise $N(0, 0.01)$ by classical operators	34
<b>Figure 2.24</b>	Edges from Boat image with Gaussian Noise $N(0, 0.01)$ by classical operators	34
<b>Figure 2.25</b>	Edges from House image with Gaussian Noise $N(0, 0.01)$ by classical operators	35
<b>Figure 2.26</b>	Edges from Camera Man image with Gaussian Noise $N(0, 0.01)$ by classical operators	35
<b>Figure 3.1</b>	Localization of the discrete wavelets in the time-scale space on a dyadic grid	48
<b>Figure 3.2</b>	Touching wavelet spectra resulting from scaling of the mother	vii

wavelet in the time domain

51

**Figure 3.3**

How an infinite set of wavelets is replaced by one scaling function

52

**Figure 3.4** Splitting the signal spectrum with an iterated filter bank 54

**Figure 3.5**

Implementation of equations 3.26 & 2.27 as one stage of an iterated filter bank

59

**Figure 4.1** Examples of the different thinning rules 64

**Figure 4.2** Lina Image decomposed in to four levels using DWT 66

**Figure 4.3** House Image decomposed in to four levels using DWT 66

**Figure 4.4** Camera man image decomposed in to four levels using DWT 67

**Figure 4.5**

Wavelet analysis filter banks and its synthesis for edge detection

69

**Figure 4.6** WSC compared with Canny edge detector 72

**Figure 4.7**

Edge map obtained by WSC, with Gaussian Noise (a) 0.02, (b) 0.05 and (c) 0.1

73

**Figure 4.8** Edge map obtained by WSC (Left) no edge enhancement (Right) Edge thinning followed by edge alignment

74

viii

## List of Acronyms

Daubach's Db

Difference of Box DoB

Difference of Gaussian DoG

Discrete Fourier Transform DFT

Discrete Wavelet Transform DWT

Distance Transform DT

Fast Wavelet Transform FWT

Fourier Transform FT

Inverse Discrete Fourier Transform IDFT

Inverse Discrete Wavelet Transform IDWT  
Hybrid Edge Detector HED  
Identity Matrix I  
Laplacian of Gaussian LoG  
Level lvl  
Mean Square Error MSE  
Multiresolution Analysis MRA  
One dimensional 1D  
Peak Signal to Noise Ratio PSNR  
Perfect Reconstruction PR  
Quadrature Mirror Filter QMF  
Short Time Fourier Transform STFT  
Signal to Noise Ratio SNR  
Two dimensional 2D  
Wavelet Scale Correlation WSC  
Wavelet Transform WT



# **Chapter 1**

## **Overview**

### **1 Introduction**

Edge detection is a first step in computer vision . Besides, its an inevitable process in image segmentation, feature extraction or scene analysis. Many approaches to image interpretation are based on edges, since analysis based on edge detection is insensitive to change in the overall illumination level. Edge detection highlights image contrast. Detecting contrast, which is difference in intensity, can emphasise the boundaries of features within an image, since this is where image contrast occurs. This is how human vision can perceive the perimeter of an object, since the object is of different intensity to its surroundings. Essentially, the boundary of an object is a step change in the intensity levels. Differencing adjacent points reveal change in intensity. Vertical edge will be marked by differencing adjacent points in horizontal direction (horizontal edge detector). Horizontal edge are detected by a a vertical edge detector which employs differencing adjacent points in vertical direction. The threshold level controls the number of selected points; too high a level can select too few points, whereas too low a level can select too much noise. Often, the threshold level is chosen by experience or by experiment.

#### **1.1 Existing Techniques on Edge detection**

The discontinuities, that is abrupt changes in pixel intensity, can be identified in spatial, frequency as well as in time-frequency domain. Each domain has distinct advantages. Spatial operators or firstorder operators are good in localization accuracy; frequency domain operators tend to bring out global information whereas time-frequency analysis is a compromise between them. First-order edge detection is based on the premise that differentiation highlights change; image intensity changes in the region of a feature boundary. The result of firstorder edge detection is a peak where the rate of change of the original signal, is greatest. There are higher order derivatives; applied to the same cross-section of data, the second-order derivative. Second-order derivative is greatest where the rate of change of the signal is greatest and zero when the rate of change is constant. The rate of change is constant at the peak of the first-order derivative. This is where there is a zero-crossing in the second-order derivative, where it changes sign. Accordingly, an alternative to first-order differentiation is to apply second-order differentiation and then find zero-crossings in the second-order

information.

A diversity of edge detectors exist which are differentiated from each other in mathematical or implementation techniques. Hence a generic edge detector is required whose performance should remain constant in most of scenarios and could captures the details required for high level processing.

3

### 1.1.1 Spatial Operators

As per Classical methods of edge detection, a 2-D filter is convolved with an image. The filter gives response to large gradients in the image and returns a zero in regions having no change in intensity. Many edge detection techniques are available [3], each designed to react differently to different edge types. Broadly, all these methods can be categorized in two classes, i.e *Gradient and Laplacian edge detectors* [1]. First-order derivative or the gradient method searches the local maximum in first derivate of the image to detect the edges. After having calculated the magnitude of the 1st derivative, pixels pertaining to boundary of an edge are marked. This is achieved by thresholding the gradient image. It is assumed that pixels, with gradients higher than the assumed threshold, are set to white (object boundaries) and those below the threshold are set black (background). A different method is to search local maxima in the gradient image. This will result an edge response of one pixel in width. An algorithmic approach to edge detection has been introduced by *Canny edge detector* [5]. Canny described a method of generating edge detectors using an optimization approach and showed how to use the technique to generate a robust detector for step edges.

The Laplacian operator is a template which implements second-order differencing. The second-order differential can be approximated by the difference between two adjacent first-order differences. Laplacian operator is an isotropic operator (like the Gaussian operator): it has the same properties in each direction. However, it lacks smoothing and will respond to noise, more so than a first-order operator since it is differentiation of a higher order. As such, the

4

Laplacian operator is rarely used in its basic form. When this is incorporated with the Laplacian we obtain a Laplacian of Gaussian (LoG) operator which is the basis of the Marr–Hildreth approach. A clear disadvantage with the Laplacian operator is that edge direction is not available. It does, however, impose low computational cost, which is its main advantage. Though interest in the Laplacian operator abated with rising interest in the Marr–Hildreth approach, a nonlinear Laplacian operator was developed and shown to have good performance,

especially in low-noise situations.

Beside noisy environment, another problem which makes edge detection a nontrivial task is *thresholding*; identification of pixels corresponding to an edge. The choice of threshold is empirical and depends upon the desired application. Further, the size of the kernel for edge detection is fixed and the user has no control over its scale. Therefore, the identification of either fine variations or smooth variations in an image is not possible through a generic spatial domain operator. The compactly supported filters fail to identify the structural variations in the image. On the other hand, large size kernels lose fidelity and localization accuracy.

### **1.1.2 Frequency Domain Filters**

Filtering is a major use of Fourier transforms [7], particularly because we can understand signal processing much better in the frequency domain. An analogy is the use of a graphic equalizer to control the way music sounds. In images, if we want to remove high frequency information (like the hiss on sound) then we can filter, or remove, it by inspecting the Fourier transform. If we retain low

5

frequency components, then we implement a low-pass filter. The low-pass filter describes the area in which we retain spectral components, the size of the area dictates the range of frequencies retained, and is known as the filter's bandwidth. If we intend to retain components within a circular region centred on the d.c. value, and inverse Fourier transform will result in blurred image. Higher spatial frequencies exist at the sharp edges of features, so removing them causes blurring. But the amount of fluctuation is reduced too; any high frequency noise will be removed in the filtered image.

### **1.2 Noise Models**

Signal and noise are basic building blocks of data analysis in the real world. The signal is usually corrupted by noise, which is often additive and is characterized by a Gaussian distribution, Poisson distribution, Rayleigh distribution, Uniform distribution or their combination. Segregation of noise and information in the signal is a challenging problem. There is a fundamental tradeoff between noise reduction and loss of information.

This thesis implements a novel edge detection paradigm in a noisy scenario with following parameters:-

- Gaussian noise has been considered with zero mean. Mat lab GUI developed to implement novel edge detector allows to vary standard deviation from 0.01 to 0.1.

- Noise is independent of the pixel values and is spatially uncorrelated; in other words it is identically independently distributed (iid).

6

### **1.3 Objectives**

A large number of spatial domain operators have been developed which are working quite satisfactorily and being widely used. They behave differently on different images and for different noise models / intensities. Their optimality in detection is achieved by manual thresholding. There is no generic threshold for edge detection that could be optimal in all scenarios. There is a need to develop a generic edge detection technique which does not require user intervention and could satisfactorily detect edges and improve the results as compared to existing techniques under a noisy scenario. Edge Detection through Wavelet Scale Correlation [11] is a new edge detection paradigm, however, edges are required to be enhanced to fill up the missing edge pixels for better results. The objective of this research work is to explore under mentioned techniques for better edge detection under the umbrella of wavelet scale correlation in a noisy scenario:-

- Adaptive thresholding instead of default/experimentally derived value.
- Interpolation of low resolution images to high resolution images.
- Image reconstruction through wavelet synthesis after processing the wavelet coefficients.
- Non maximal suppression
- Techniques for capturing missing edge pixels / edge linking.

7

### **1.4 Author's Contribution**

The contribution of the author in the chosen field of research is summarized as below.

- i. Novel wavelet synthesis has been developed such that the reconstructed image fabricates the image edge map.
- ii. Adaptive thresholding of low resolution images, formed during image decomposition through wavelet scale correlation, based on a value derived through mean and standard deviation of the image.
- iii. Interpolation techniques have been explored. Since each decomposed image is being thresholded based on its statistical

parameters. The interpolation technique could be better to use in image reconstruction to obtain an edge map with merits and demerits have been discussed.

iv. Wavelet Scale Correlation is a new edge detection paradigm. Edge map obtained after image synthesis has been processed further, since the edges become thick during interpolation. Various edge enhancement methods such as used by Canny have been explored.

## **1.5 Thesis Organisation**

Chapter 1 defines the edge detection, formulates the problem for classical edge detectors and highlights the objectives of the thesis.

8

Chapter 2 reviews the edge detectors in general and encompasses both gradient and Laplacian operators. Highpass filtering through Fourier analysis is highlighted. Implementation of spatial and frequency domain operators have been shown on standard (bench) images and their inability to extract edge maps of the images under depleted signal to noise ratio (SNR) has been demonstrated. The inability of classical edge detectors to extract good edge maps of the images under standard threshold values is envisaged.

Chapter 3 builds up the theory of WT and develops its implementation for edge detection. Subband coding and actual implementation of DWT through MRA has been discussed.

Chapter 4 presents a novel wavelet synthesis based on WSC of concordant detail bands such that the reconstructed image yields image edge map. The proposed scheme is compared with spatial domain classical edge detectors, frequency domain operators. The chapter concludes the thesis and indicates areas of further research.

9

## ***Chapter 2***

### **Classical Edge Detectors**

#### **2.1 Edge Detection**

The first problem encountered in Edge Detection is defining what is an *edge*. Edges, being step discontinuities in the image intensities, can be recognized by finding local maxima in the first derivative [13], or zero-crossings in the second derivative of the image. This idea was first suggested by David Marr, and later developed by Marr and Hildreth [14], and many others [2].

Finding local maxima in the first derivative requires differencing between the pixels intensities next to and behind the pixel under consideration. Areas of constant intensities yield a zero and are thus suppressed. All results including any

number greater or smaller than zero is saved in a separate image, which represents parts of the image where changes occur in pixel intensities and parts of the images where there is no change at all.

Edge detection schemes suffer from a number of problems. The main problem is thresholding which is a function of edge properties, characteristics of smoothing filter and properties of differential operators [12]. In order to detect the edges of buildings from an image or to detect the boundaries of bricks of the buildings from the same image need different edge detection threshold. Further, noise severely affects the choice of threshold. Thus thresholding makes edge

10

detection a non trivial task as it varies from image to image [17]. Each operator behaves differently for different thresholds and for different noise models. The choice of the size of a filter is a compromise between sensitivity to noise and fine localization. A large filter is less sensitive to noise but lacks edge localization accuracy as compared to small filter.

## 2.2 Spatial Domain Filters

Various edge detection techniques in spatial domain can be classified in to two classical algorithms. The first is gradient and second is Laplacian. Popular among gradient operators [1], [2] are Robert, Sobel, Prewitt, Frei-Chen. Among Laplacian, popular operators include Laplacian and Laplacian of Gaussian (LoG).

The gradient method is common and simple operator that detects edges by finding local maxima in the first derivative of the image. Finding local maxima in the first derivative requires differencing between the pixels intensities next to and behind the pixel under consideration. Areas of constant intensities yield a zero and are thus suppressed. All results including any number greater or smaller than zero is saved in a separate image, which represents parts of the image where changes occur in pixel intensities and parts of the images where there is no change at all. A graph showing changes in pixel intensities is shown in figure 2.1. Where the rate of change is maximum, first derivate will show a maxima or location of edge. Calculating the 2<sup>nd</sup> derivate of the image can highlight its location showing zero crossing at the location of maxima in first derivate [18].

11

**Figure 2.1** Edge Detection through First and Second Derivative operators

### 2.2.1 Gradient Operators

Consider a gradient image  $g(x,y)$  computed by storing the gradient magnitudes resulting from differencing operation on both x and y coordinates of the image.

Mathematically:-

$$g(x,y) = \sqrt{(\frac{\partial I}{\partial x})^2 + (\frac{\partial I}{\partial y})^2}$$

□

## 2.1

where,  $\Delta x = \frac{I(x+1, y) - I(x-1, y)}{2}$ ,  $\Delta y = \frac{I(x, y+1) - I(x, y-1)}{2}$ . In

order to reduce the computational complexity, the gradient is approximated as

$$|\nabla I| \approx \max(|\Delta x|, |\Delta y|) \quad (2.2)$$

Consider  $\theta(x, y)$  as the gradient direction and can be calculated as :-

12

$$\theta(x, y) = \tan^{-1} \frac{\Delta y}{\Delta x}$$

$\Delta x$

$\Delta y$

## 2.3

$\Delta x$  and  $\Delta y$  can be implemented by aligning a 3 x 1 mask with values -1 0 1 with image in x and y axes. To increase the localization accuracy, a 3 x 3 masks ( $G_x$  and  $G_y$ ) are used to calculate  $\Delta x$  and  $\Delta y$ . The **Gx** and **Gy** masks shown in figure 2.2.

1 2 1 -1 0 1

0 0 0 -2 0 2

-1 -2 -1 -1 0 1

$G_x$   $G_y$

**Figure 2.2** Horizontal and Vertical 3 x3 Convolution masks

The kernel origin is located at the center value and the arrows indicate the direction that each kernel measures. That is,  $G_x$  calculates  $\Delta x$  and detects horizontal edges, and  $G_y$  calculate  $\Delta y$  and detects vertical edges. Edge direction is considered to be perpendicular to the direction of operation while calculating  $G_x$  and  $G_y$ . If the sum of pixel intensities in a region in the image results a non zero while calculating  $G_x$ , a horizontal edge is detected. Similarly a non zero value in a region while calculating  $G_y$  indicates a vertical edge.

Using equation 2.2 gradient magnitude are calculated. Gradient magnitude indicates the difference between pixel's intensities in the neighborhood. Angles of edges are computed using equation 2.3. Both the magnitude and angles of edges are usually stored as two separate image frames.

13

### 2.2.1.1 Sobel Gradient Operator

The operator consists of a pair of 3x3 convolution kernels as shown in Figure 2.2. One kernel is simply the other rotated by 90°. These kernels [8] are designed to respond maximally to edges running horizontally and vertically relative to the pixel grid, one kernel for each of the two perpendicular orientations.

### 2.2.1.2 Prewitt Gradient Operator

Figure 2.4 shows horizontal and vertical Prewitt operators.

```
1 1 1 -1 0 1
0 0 0 -1 0 1
-1 -1 -1 -1 0 1
Gx □ Gy □
```

**Figure 2.4** Prewitt Kernels

The sole difference between Sobel and Prewitt lie in the weighting of the middle row/column, vertical and horizontal kernels respectively. Sobel uses a weighting of 2/-2 whereas Prewitt makes use of 1/-1. This results in smoothing since there is more importance to the centre point so it is evident that Sobel operator is more immune to noise as compared to Prewitt operator.

### 2.2.1.3 Robert's Cross Operator

Both Sobel and Prewitt are sensitive to horizontal and vertical edges. Robert presents variation to this scheme by introducing a pair of 2 x 2 mask as shown in figure 2.5. These masks are designed to respond well to diagonal edges as compared to Sobel and Prewitt.

```
14
1 0 0 1
0 -1 -1 0
```

**Figure 2.5** Robert's cross Kernels

One kernel is simply the other rotated by 90°. Being compact, Robert's Cross operator results in lesser calculations. It gains in execution speed and loses fidelity because of its compact support. Its disadvantage is sensitivity to noise and localization errors [3].

### 2.2.2 Second Derivative Operators

First-order edge detection is based on the premise that differentiation highlights change; image intensity changes in the region of a feature boundary. Where rate of change is maximum, 1<sup>st</sup> derivative shows a maxima in the graph between  $f(x)$  and  $x$  axis of the image resulting a peak. The second-order derivative is greatest where the rate of change of the intensity is greatest and zero when the rate of change is constant. The rate of change is constant at the peak of the first-order derivative. This is where there is a zero-crossing in the second-order derivative, where it changes sign. Accordingly, an alternative to first-order differentiation is to apply second-order differentiation and then find zero-crossings in the second-order information.

#### 2.2.2.1 Laplacian Operator

The Laplacian operator is a template which implements second-order differencing. The second-order differential can be approximated by the difference



between two adjacent first-order differences [20]:

$$\begin{bmatrix} 1 & 2 & -1 \\ 2 & 5 & -2 \\ -1 & -2 & 1 \end{bmatrix} \quad 2.4$$

15

$$\begin{bmatrix} 1 & 2 & -1 \\ 2 & 5 & -2 \\ -1 & -2 & 1 \end{bmatrix}$$

$$\begin{bmatrix} 1 & 2 & -1 \\ 2 & 5 & -2 \\ -1 & -2 & 1 \end{bmatrix} - \begin{bmatrix} 1 & 2 & -1 \\ 2 & 5 & -2 \\ -1 & -2 & 1 \end{bmatrix}$$

$$\Delta^2$$

2.5

$$\begin{bmatrix} 1 & 2 & -1 \\ 2 & 5 & -2 \\ -1 & -2 & 1 \end{bmatrix} \quad 2.6$$

This gives a horizontal second-order template as

$$-1 \ 2 \ -1$$

When the horizontal second-order operator is combined with a vertical second-order

difference we obtain the full Laplacian template, given in figure 2.6

$$0 \ -1 \ 0$$

$$-1 \ 4 \ -1$$

$$0 \ -1 \ 0$$

**Figure 2.6** Laplacian Template

An alternative structure to the template in figure 2.6 is one where the central weighting is 8 and the neighbors are all weighted as  $-1$ . This includes a different form of image information, so the effects are slightly different. In both structures, the central weighting can be negative and that of the four or the eight neighbors can be positive. The only key is the sum of values in the mask must be zero, so that areas of constant intensities could be suppressed. One advantage of the Laplacian operator is that it is isotropic (like the Gaussian operator): it has the same properties in each direction. However, it contains no smoothing and will respond to noise more than a first-order operator since it is differentiation of a higher order.

The Laplacian operator is rarely used in its basic form. Smoothing can be used by the averaging operator but a more optimal form is Gaussian smoothing.

16

When this is incorporated with the Laplacian of Gaussian (LoG) operator is obtained which is the basis of the Marr–Hildreth [4],[22] approach, to be considered next. A clear disadvantage with the Laplacian operator is that edge direction is not available. It does, however, impose low computational cost, which is its main advantage.

### 2.2.2.2 The Marr–Hildreth operator

$$\begin{bmatrix} 1 & 2 & -1 \\ 2 & 5 & -2 \\ -1 & -2 & 1 \end{bmatrix} \quad 2.7$$

where

Figure 2.8, Laplacian of Gaussian operator

### 2.8

By differentiation w.r.t x and y:-

Figure 2.8, Laplacian of Gaussian operator

Figure 2.8, Laplacian of Gaussian operator

Figure 2.8, Laplacian of Gaussian operator

Figure 2.8, Laplacian of Gaussian operator

### 2.9

Equation 2.9 shows how to calculate the values of a mask which is a combination of 1st order differentiation and Gaussian smoothing. When equation 2.9 is again differentiated, it gives Laplacian of Gaussian (LoG) operator:

Figure 2.9, Laplacian of Gaussian operator

Figure 2.9, Laplacian of Gaussian operator

### 2.10

17

The operator is shown in figure 2.7 and is called a 'Mexican hat' operator, since its surface plot is the shape of a sombrero.

Figure 2.7 Shape of Laplacian of Gaussian operator and its discrete approximation with 3x3 mask

### 2.2.3 Canny's Edge Detection Algorithm

Canny went on designing a optimal edge detection paradigm using existing edge detectors [15]. Canny followed following criterion to improve current methods of edge detection [19]:-

- **Low error rate.** There should be no response to false edges. Similarly there must be a response to true edges
- **Localization Accuracy.** Unlike a step change in pixel intensities which can be considered as a ideal edge, a smooth edge has series of changes that are many pixel wide. To mark an location is critical. The distance between the actual edge and marked edge is called localization error and is required to be minimized.

18

- **One response to a single edge.** As it can be seen, directional operators will always respond to a single pixel edge with three pixels. Canny ensured that there must be one reponse to any edge.

With these objectives in mind Canny devised an edge detection paradigm as follows:-

- Gaussian smoothing to reduce noise.

- Calculating image gradients in both x and y directions using Sobel masks and calculating gradient magnitudes and directions.
- Relating Edge Directions. Once the edge direction is calculated it is related to a direction that can be traced in an image.
- Tracks along gradients in the related direction of edge and suppresses any pixel that is not at the maximum (non-maximum suppression).

19

### **2.2.3.1 Step 1: Noise Suppression**

In order to implement Canny edge detector algorithm, a series of steps must be followed. The first step is to filter out any noise in the original image before trying to locate and detect any edges. And because the Gaussian filter can be computed using a simple mask, it is used exclusively in the Canny algorithm. Once a suitable mask has been calculated, the Gaussian smoothing can be performed using standard convolution methods. A convolution mask is usually much smaller than the actual image. As a result, the mask is slid over the image, manipulating a square of pixels at a time. The larger the width of the Gaussian mask, the lower is the detector's sensitivity to noise. The localization error in the detected edges also increases slightly as the Gaussian width is increased.

### **2.2.3.2 Step 2: Calculating Edge Strength by Taking the Gradient**

After smoothing the image and eliminating the noise, the next step is to find the edge strength by taking the gradient of the image. The Sobel operator performs a 2-D spatial gradient measurement on an image. Then, the approximate absolute gradient magnitude (edge strength) at each point can be found.

### **2.2.3.3 Step 3: Direction of Edge**

The direction of edge is computed using the gradient in the x and y directions. Whenever the gradient in the x direction is equal to zero, the edge direction has to be equal to 90 degrees or 0 degrees, depending on what the value of the gradient in the y-direction is equal to. If  $G_y$  has a value of zero, the edge direction will equal 0 degrees. Otherwise the edge direction will equal 90 degrees.

## **2.2.3**

Once

a dir

align

whe

**45 d**

**135**

reso

close

degr

degr

67.5

to 1

**regio**

**3.4 St**

e the edge

rection tha

ned as show

It can be

n describi

**degrees** (al

**degrees** (

lved into

est to (e.g

rees). Figur

Any edg

rees) is set

degrees)

12.5 degre

**on 4** (112.5

**tep 4: Rela**

e direction

at can be

wn in figur

e seen by l

ng the sur

ong the po

along the

one of th

g. if the or

re 2.9 expl

ge directio

t to 0 deg

is set to 45

ees) is set

5 to 157.5

## ating Edge

is known,  
traced in  
re 2.8

### Fig

ooking at  
rounding  
ositive diag  
negative d  
hese four  
rientation  
ans the co

### Figur

on falling w  
grees. Any  
5 degrees.  
to 90 deg  
degrees) i  
20

## e Direction

, the next  
an image

```
x x x x  
x x x x  
x x A x  
x x x x  
x x x x
```

### gure 2.8

5x5  
pixel "a", t

pixels - **0**

gonal), **90**

diagonal).

directions

angle is f

oncept:-

### re 2.9

Edge D

within the

edge dire

. Any edge

grees. And

s set to 13

**ns**

step is to

. So if the

x

x

x

x

x

image

there are 0

**degrees** (i

**degrees** (

Now the

s dependin

found to b

Directions

**region 1**

ection falli

e direction

any edge

35 degrees

relate the

e pixels of

only four p

in the hor

in the vert

edge orien

ng on whi

be 3 degree

(0 to 22.5

ng in the

falling in t

direction

.

edge direc

a 5x5 ima

possible dir

izontal dir

tical direct  
ntation ha  
ich directi  
ees, make  
5 & 157.5  
**region 2** (  
the **region**  
falling wit  
ction to  
age are  
rections  
ection),  
tion), or  
as to be  
on it is  
it zero  
to 180  
22.5 to  
**3** (67.5  
thin the  
21

### **2.2.3.5 Step 5: Non-Maximum Suppression**

After the edge directions are known, non-maximum suppression has to be applied. Non-maximum suppression is used to trace along the edge in the edge direction and suppress any pixel value (sets it equal to 0) that is not considered to be an edge. This will give a thin line in the output image.

### **2.2.3.6 Step 6: Hysteresis**

Hysteresis is used as a means of eliminating streaking which is the breaking up of an edge contour caused by the operator output fluctuating above and below the threshold. If a single threshold, T1 is applied to an image, and an edge has an average strength equal to T1. Due to noise, there will be instances where the edge dips above or below the threshold making an edge look like a dashed line. To avoid this, hysteresis uses 2 thresholds, a high and a low; T1 and T2 respectively. Value greater than T1 is presumed to be an edge pixel, and is marked as such. Pixels below T2 are set to zero. Then, any pixels that are connected to this edge pixel and that have a value greater than T2 are also selected as edge pixels.

## **2.2.4 Implementation of Classical Operators**

Edges detected from Bench mark images (attached at Appendix A) that include Lena, Building, Boat, House and Cameraman through gradient and second derivate operators are shown in figures 2.10 to 2.14.

22

**Figure 2.10** Edges detected from Lena image by conventional operators

**Figure 2.11** Edges detected from Building image by conventional operators

23

**Figure 2.12** Edges detected from Boat image by conventional operators

**Figure 2.13** Edges detected from House image by conventional operators

24

**Figure 2.14** Edges detected from Camera Man image by conventional operators

## 2.2.5 Performance of Edge Detection Algorithms

The figures 2.10 to 2.14 demonstrate the edge detection results of classical edge detectors. The behavior of the operators is consistent in all the figures. Few true edges are found missing in gradient operators whereas false edges are cluttered in second derivative operators. Although, Canny takes on an algorithmic approach for edge detection, yet dominance of false edges can be visualized in the above figures. The false edges are more prominent for high frequency images such as Boat image. The results are further deteriorated under noisy scenario that will be demonstrated in section 2.4.2. The good edge detection results depend upon selecting an appropriate threshold that is empirical.

25

## 2.3 Frequency Domain Filters

Changes in intensities in an image canalso be computed in frequency domain using Fourier Analysis. Since edge are high frequency contents, a high pass filter will simply extract the desired edges in the image. Fourier transform and inverse Fourier transforms are defined [1] as

$$F(u, v) = \int_{-\infty}^{\infty} \int_{-\infty}^{\infty} f(x, y) e^{-j2\pi(ux + vy)} dx dy$$

$$f(x, y) = \int_{-\infty}^{\infty} \int_{-\infty}^{\infty} F(u, v) e^{j2\pi(ux + vy)} du dv$$

$$F(u, v) = \int_{-\infty}^{\infty} \int_{-\infty}^{\infty} f(x, y) e^{-j2\pi(ux + vy)} dx dy$$

### 2.11

$$F(u, v) = \int_{-\infty}^{\infty} \int_{-\infty}^{\infty} f(x, y) e^{-j2\pi(ux + vy)} dx dy$$

$$f(x, y) = \int_{-\infty}^{\infty} \int_{-\infty}^{\infty} F(u, v) e^{j2\pi(ux + vy)} du dv$$

$$F(u, v) = \int_{-\infty}^{\infty} \int_{-\infty}^{\infty} f(x, y) e^{-j2\pi(ux + vy)} dx dy$$

### 2.12

Our interest is in discrete functions, so we will dwell on Fourier transform of discrete functions. Equation 2.13 gives Discrete Fourier Transform (DFT) of a two dimensional function f(x,y).

$$F(u, v) = \sum_{x=0}^{M-1} \sum_{y=0}^{N-1} f(x, y) e^{-j2\pi(ux + vy)}$$

$$f(x, y) = \frac{1}{MN} \sum_{u=0}^{M-1} \sum_{v=0}^{N-1} F(u, v) e^{j2\pi(ux + vy)}$$

$$\Sigma \Sigma_{x=0}^{M-1} \Sigma_{y=0}^{N-1} f(x, y) e^{-j2\pi(ux + vy)}$$



2 22222222

2 222

2 222 2

2 2.13

for  $x=0,1,2,\dots,M-1$  and  $y=0,1,2,\dots,N-1$ .

222, 22 2 222, 22 2 222, 22222, 22 2.14

222, 22222, 22 2 222, 22 2 222, 22 2.15

26

Edge detection in frequency domain is straight forward as shown in figure 2.15 through high-pass filtering as following:

- Compute DFT of the input image.
- Centre shift the frequencies.
- Multiply the  $F(u,v)$  by a filter function  $H(u,v)$ .
- Un-shift the frequencies.
- Compute IDFT of step 4

**Figure 2.15** Edge detection in frequency domain

Edges can be considered as transients in a signal or mathematically defined as local singularities. The Fourier transform is global in behavior and not well adapted to identify sharp transients.

27

**Figure 2.16** Edges detected by highpass filtering from bench images.

(a) Lena. (b)House. (c) Cameraman.

## 2.4 Effects of Noise on Edge Detection

Noise in digital images arise during image acquisition and/or transmission. During acquisition, various factors to include environmental conditions and quality of the sensing elements affect the imaging sensors. During transmission, images are subject to interference in the channel used [1],[24].

Spatial characteristics of noise show whether or not the noise is correlated with the image. Frequency properties refer to the frequency content of noise in the Fourier sense.

### 2.4.1 Noise models

Various types of noise present in images are photon, thermal and quantization noise etc. Photon and thermal noise can be reduced effectively by using accurate and controlled 'sensing' devices. Quantization noise can be reduced by considering additional quantization levels. The error rate thus is reduced and is not very significant. The classification of noise is based upon the shape of the probability density function or histogram for the discrete case of the noise.

### 2.4.1.1 Gaussian Noise

Because of its mathematical tractability in both the spatial and frequency domains, Gaussian (also called normal) noise models are used frequently in practice. In fact, this tractability is so convenient that it often results in Gaussian models being used in situations in which they are marginally applicable at best. The PDF of a Gaussian random variable,  $z$ , is given by

$$p(z) = \frac{1}{\sqrt{2\pi}\sigma} e^{-\frac{(z-\mu)^2}{2\sigma^2}} \quad (2.16)$$

where

$$\mu = \text{mean of } z$$

$\sigma$  is its

$$\sigma = \text{standard deviation}$$

Figure 2.17

where 'z' represents gray level,  $\mu$  is the mean of average value of  $z$ , and  $\sigma$  is its standard deviation. A plot of this function is shown in figure 2.17. When 'z' is described by equation 2.16, approximately 63% of its values will be in the range  $\mu - \sigma$ ,  $\mu + \sigma$ , and about 95% will be in the range  $\mu - 2\sigma$ ,  $\mu + 2\sigma$ .

**Figure 2.17** Probability Density Function of Gaussian Noise

29

### 2.4.1.2 Rayleigh Noise

The PDF of Rayleigh noise is given by

$$p(z) = \frac{2z}{b^2} e^{-\frac{z^2}{b^2}} \quad (2.17)$$

where

$b$  is

$$b = \sqrt{2a}$$

$a$  is the

$$a = \frac{b^2}{2}$$

Figure 2.17

The mean and variance of this density are given by

$$\mu = \frac{a}{\sqrt{2}}$$

$\sigma^2 = \frac{4}{\pi^2} b^2$

Figure 2.18

and

$\sigma^2 = \frac{4}{\pi^2} b^2$

Figure 2.19

$$b^2 = \frac{4}{\pi^2} \sigma^2$$

Figure 2.19

Figure 2.19

Figure 2.18 shows a plot of the Rayleigh density. Note the displacement from the origin and the fact that the basic shape of this density is skewed to the right. The Rayleigh density can be quite useful for approximating skewed histograms.

**Figure 2.18** Probability Density Function of Rayleigh Noise

30

### 2.4.1.3 Exponential Noise

The PDF of exponential noise is given by

$$p(z) = \begin{cases} a e^{-az} & \text{for } z \geq 0 \\ 0 & \text{for } z < 0 \end{cases}$$

where  $a > 0$ .

The mean and variance of this density function are

$\mu = \frac{1}{a}$

$$\sigma^2 = \frac{1}{a^2}$$

and

$$\sigma^2 = \frac{2}{a^2}$$

Figure 2.19 shows a plot of this density function.

**Figure 2.19** Probability Density Function of Exponential Noise

### 2.4.1.4 Uniform Noise

The PDF of uniform noise is given by

The

and

Figure

### 2.4.1

The

mean of th

its varianc

re 2.20 sho

### 1.5 Im

PDF of (bip

his density

ce by

ows a plot

**Figure 2**

### mpulse (Sa

polar) imp

y function i  
of the uni

2.20 Probabil

### **It-and-Pep**

ulse noise

31

is given by

form dens

ity Density Fu

### **pper) Nois**

is given by

sity.

unction of Un

**e**

y

niform Noise

32

If  $b > a$ , gray-level  $b$  will appear as a light dot in the image. Conversely, level  $a$  will appear like a dark dot. If either  $P_a$  or  $P_b$  is zero, the impulse noise is called unipolar. If neither probability is zero, and especially if they are approximately equal, impulse noise values will resemble salt-and-pepper granules randomly distributed over the image. For this reason, bipolar impulse noise also is called salt-and-pepper noise. Shot and spike noise also are terms used to refer to this type of noise.

**Figure 2.21** Density Function of Impulse Noise

Figure 2.21 shows the PDF of impulse noise. Noise impulses can be negative or positive. Scaling is part of the image digitizing process. Because impulse corruption is large compared with the strength of the image signal, impulse noise generally is digitized as extreme (pure black or white) values in an image; both  $a$  and  $b$  are "saturated" values. They are equal to the minimum and maximum allowed values in the digitized image. As a result, negative impulses appear as black (pepper) points in an image and positive impulses appear white (salt) noise.

33

### **2.4.2 Implementation of Classical Operators under Noisy Scenario**

Similarly edges detected from noisy bench mark images that include Lena, Building, Boat, House and Cameraman through gradient and second derivate operators that include Sobel, Prewitt, Robert, Laplacian, LoG and Canny edge detectors are shown in figures 2.22 to 2.26 with Guassian noise induced in the

images is Gaussian with zero mean and variance of 0.01. Figure 2.27 to 2.31 are results with Gaussian noise of zero mean and variance of 0.02.

These results can be compared with figures 2.10 to 2.14 and will be referred back in the subsequent chapters for comparison of the results.

**Figure 2.22** Edges from Lina image with Gaussian Noise  $N(0, 0.01)$  by classical operators  
34

**Figure 2.23** Edges from Building image with Gaussian Noise  $N(0, 0.01)$  by classical operators

**Figure 2.24** Edges from Boat image with Gaussian Noise  $N(0, 0.01)$  by classical operators  
35

**Figure 2.25** Edges from House image with Gaussian Noise  $N(0, 0.01)$  by classical operators

**Figure 2.26** Edges from Camera Man image with Gaussian Noise  $N(0, 0.01)$  by classical operators  
36

**Figure 2.27** Edges from Lina image with Gaussian Noise  $N(0, 0.02)$  by classical operators

**Figure 2.28** Edges from Building image with Gaussian Noise  $N(0, 0.02)$  by classical operators  
37

**Figure 2.29** Edges from Boat image with Gaussian Noise  $N(0, 0.02)$  by classical operators

**Figure 2.30** Edges from House image with Gaussian Noise  $N(0, 0.02)$  by classical operators  
38

**Figure 2.31** Edges from Camera Man image with Gaussian Noise  $N(0, 0.02)$  by classical operators

## 2.5 Conclusion

The classical edge kernels are predetermined and lack control over its scale for edge detection. The edge detectors are unable to adequately grab moderate intensity variations in the image. These kernels are highly localized and have compact support. Another problem is lack of standard thresholds for edge detection. A good threshold for one image may exhibit verborisities for other image. It is therefore difficult to obtain optimum edge detection results without user's intervention for inputting parameters for the edge operator. Hence it lacks automation and cannot be elegantly used in segmentation or in any other preprocessing stage in image processing applications. The derivative operators are not well immune to noise, especially second derivative operators, and hence  
39

do not give adequate edge maps of the images in noisy scenario. On the other hand Fourier transform is global in nature and not well adapted to local singularities detection. Further that for images with low SNR, high-pass filtering cannot distinguish between true and false edges. Threshold is usually empirical and its value is a tradeoff between noise elimination and extraction of true edges. Therefore there is a need to build edge operators that do not require user's intervention for inputting the parameters to obtain the desired results. Further that the size of the kernels are fixed. Small scale kernels are good for detecting fine variations and coarse scale operator extracts coarse variations. Thus the scalability in edge kernels is another issue that can be resolved through MRA

which is the subject of next chapter.

40

## ***Chapter 3***

### **Wavelets and Edge Detection**

#### **3 Introduction**

The theory of wavelets can be approached through vector spaces, signal processing or by lifting algorithms [6]. The name wavelet implies that they should integrate to zero and wave above and below the horizontal axis with compact support. Wavelets can be considered as functions that satisfy certain mathematical requirements. The biggest gain with wavelets is that they are localized in frequency and the space domains simultaneously, thus present stable representations in both domains. WT exhibits a compromise between time and frequency domain. The advantage they offer for edge detection is their ability to accurately locate the discontinuities in the image function. The fact that the edges are nothing but the high frequency contents of the image have given the basis for the use of wavelets for edge detection.

#### **3.1 Historical Perspective**

The road towards the wavelets started with Josef Fourier with his research on frequency analysis. The term wavelets was first mentioned by Haar in 1909 and introduced compactly supported Haar wavelet. However, it was not perceived at that time that the wavelets will be established so strongly in mathematics, modern physics and engineering disciplines. The researchers in 1930 molded the

41

research direction [26] from frequency analysis into scale analysis. Paul Levy found that in order to investigate small and complex details, Haar has more flexible and advantageous basis over Fourier.

Littlewood, Paley, and Stein proved the energy conservation of the signal is domain independent led Davis Mar in 1980 to introduce an effective way to use numerical integration. The theory of wavelets can be evolved from different approaches. Fourier transform constitutes fixed bases with infinite support. It is localized in frequency but does not provide space or time information of the signal. The widening approach of Fourier transform known as short time Fourier transforms (STFT) is a tradeoff between localization of frequency and time. It does not give flexibility to application to change the resolution as per requirements. Therefore, it is not well adapted to isolate local singularities. It leads to more general and flexible approach in which analysis at different resolution and details can be made. A function can be analyzed by taking its projection on a single prototype function along its translations and scaling such that the prototype

function obeys certain mathematical criteria. This phenomenon results in CWT. If the said basis function is discretized and then the signal is analyzed, it is termed as

42  
discrete time wavelet transforms. If the translations are integer multiples of two then it results in well known dyadic wavelet transform. Another approach is based on multiresolution approach which states that any lower dimensional signal can be represented by its higher dimension or a higher dimensional signal can be represented by lower dimension signal along its orthogonal complement. The appeal of such an approach known as MRA facilitates retention of structural contents that might go undetected at one resolution may be easy to spot at another. However wavelets could not be effectively used till Mallat discovered that dyadic wavelets can be implemented by filter banks. Implementation of wavelets has its roots in subband coding. In the subsequent sections each aspect of wavelets will be briefly touched and then its implementation for edge detection will be envisaged.

### 3.2 Short Time Fourier Transform

Fourier analysis is a useful tool to study stationary periodic signals and is not effective to study small changes in dynamic changing signals. STFT analysis a part of the signal under a fixed width window and carry out a Fourier analysis. The window is then translated and process is repeated again. This results in localized information regarding frequency contents in the signal. The problem with STFT is that its window width remains constant for all frequencies. Fourier and inverse fourier transform of a signal,  $x(t)$  are defined by the following two equations:

$$X(f) = \int_{-\infty}^{\infty} x(t) e^{-j2\pi ft} dt \quad 3.2$$

??

??

43

$$x(t) = \int_{-\infty}^{\infty} X(f) e^{j2\pi ft} df \quad 3.3$$

??

??

In reality, some portions of non-stationary signals can be found stationary. Signal is analyzed through a window, which is of the size of the stationary part of the signal. Narrow windows are required if the signal of interest is very small. This approach of researchers ended up with a revised version of the Fourier transform, STFT. STFT can be mathematically defined as

$$STFT(x, t, \omega) = \int_{-\infty}^{\infty} x(\tau) \omega(\tau - t) e^{-j\omega\tau} d\tau$$

??

??

$$\int_{-\infty}^{\infty} \omega(\tau) d\tau = 1 \quad 3.4$$

The function  $\omega(t)$  is a windowing function, the simplest of which is a

rectangular window that has a unit value over a finite interval and is zero elsewhere.

44

### 3.3 Continuous Wavelet Transform (CWT)

Unlike a sinusoidal function, a wavelet is a small wave whose energy is concentrated in time. Wavelets are functions generated from one single function called mother wavelet by dilatations and translations in time domain. A wavelet denoted by  $\Psi(t)$  should have zero average value and unit energy. Equation 3.5 shows the continuous wavelet transform of a signal  $x(t)$ :-

$$\int_{-\infty}^{\infty} x(t) \psi\left(\frac{t-b}{a}\right) \frac{1}{\sqrt{|a|}} dt$$

1

$\sqrt{s}$

$$\int_{-\infty}^{\infty} x(t) \psi\left(\frac{t-b}{a}\right) \frac{1}{\sqrt{|a|}} dt$$

$$\int_{-\infty}^{\infty} x(t) \psi\left(\frac{t-b}{a}\right) \frac{1}{\sqrt{|a|}} dt \quad 3.5$$

45

Thus the wavelet transform of a signal is computed as a collection of inner products of the signal and translated and scaled versions of a mother wavelet  $\psi(t)$ .

### 3.4 Wavelet Properties

The most desired conditions of wavelets are the *admissibility* and the *regularity*

46

47

From the admissibility condition 0th moment  $\int_{-\infty}^{\infty} \psi(t) dt = 0$ , so that the first term in the right-hand side of Equation 3.13 is zero. If the other moments up to  $\infty$  are

48

**Figure 3.1** Localization of the discrete wavelets in the time-scale space on a dyadic grid.

49

50

51

**Figure 3.2** Touching wavelet spectra resulting from scaling of the mother wavelet in the time domain.

52

**Figure 3.3** How an infinite set of wavelets is replaced by one scaling function

53

### 3.8 Subband Coding

The wavelets could not be effectively implemented in signal processing applications till its linkage with subband coding was explored. In this scheme, the image is decomposed into a set of band limited components, called subbands. The decomposition is performed in a manner such that the decomposed bands can be inverted back to re-construct the original signal without error. The decomposed signal is decimated such that it retains same number of data points



after decimation as the original signal. Each decomposed band is separately upsampled and filtered in such a way that their combination yields back the original signal or in other words the combination of lower dimensional space can generate the next higher dimensional space. For this purpose; the transfer

54

function of the system should be unity i.e. the synthesis filter bank should be the inverse of the analysis filter bank. The process of splitting the spectrum is graphically displayed in figure 3.4.

**Figure 3.4** Splitting the signal spectrum with an iterated filter bank

Another way to say is to factorize unity into two factors. One factor can correspond to coefficients of analysis filter bank and the other factor can correspond to synthesis filter bank. However these factors are constrained by certain mathematical conditions. There is no set procedure or derivations for finding these factors. The factors may be termed as magic numbers fulfilling the mathematical conditions such as compact support and orthogonality or biorthogonality in order to be successful candidate for wavelets. Consider two channel perfect reconstruction filter bank as shown in Figure 3.4. The analysis filter bank consists of  $h_0[n]$  and  $h_1[n]$ , is used to break the input sequence  $f[n]$  into two half length sequence  $f_{lp}[n]$  and  $f_{hp}[n]$ , the subbands that represents the input. The  $h_0[n]$  and  $h_1[n]$  are half band filters. Filter  $h_0[n]$  is a lowpass filter

55

whose output, subband  $f_{lp}[n]$ , is called an approximation of  $f[n]$  while  $h_1[n]$  is a highpass filter whose output, subband  $f_{hp}[n]$ , is called high frequency or detail part of  $f[n]$ . These filters are power complementary and FIR Each band is decimated by of two so that the amount of data should coincide with original signal. For synthesis the signal is up sampled by a factor of two by inserting zeros in between consecutive samples. Then it is passed to synthesis filters separately and then combined to re-construct the signal.

Summarizing, if the wavelet transform has been implemented as an iterated filter bank, the wavelets are not specified explicitly.

56

Figure 3.20 shows the decomposition of a signal  $f[n]$  into two subbands  $f_{lp}[n]$  and  $f_{hp}[n]$  using the analysis filter bank  $h_0[n]$  and  $h_1[n]$ . The subband  $f_{lp}[n]$  is the approximation of  $f[n]$  and  $f_{hp}[n]$  is the detail part of  $f[n]$ .

### 3.20

57

Figure 3.24 shows the reconstruction of a signal  $f[n]$  from its subbands  $f_{lp}[n]$  and  $f_{hp}[n]$  using the synthesis filter bank  $g_0[n]$  and  $g_1[n]$ .

Figure 3.25 shows the reconstruction of a signal  $f[n]$  from its subbands  $f_{lp}[n]$  and  $f_{hp}[n]$  using the synthesis filter bank  $g_0[n]$  and  $g_1[n]$ .

58

Figure 3.26 shows the reconstruction of a signal  $f[n]$  from its subbands  $f_{lp}[n]$  and  $f_{hp}[n]$  using the synthesis filter bank  $g_0[n]$  and  $g_1[n]$ .

2

3.27

59

**Figure 3.5** Implementation of equations 3.26 & 2.27 as one stage of an iterated filter bank.

60

### 3.10 Edge Detection

The image is passed through transform analysis filter bank that constitutes two separate one dimensional transforms. Firstly the image is filtered along horizontal axis using lowpass and highpass analysis filters that split image into two bands followed by decimation by two.

The lowpass filter corresponds to an averaging operation, extracts the coarse information of the signal. The highpass filter corresponds to differencing operation, extracts the detail information of the image.

**Figure 3.6** Image Synthesis

Finally the image has been split into four bands i.e. approximations, horizontal details, vertical details and diagonal details and are denoted by LL, HL, LH and HH respectively as shown in figure 3.6. The decomposition steps constitute the level one or the first scale decomposition. Image edge map can be obtained in the lower resolution by adding all the detail bands. The processed image is reverted back to its original dimension by upsampling followed by interpolation. The detail

61

bands are synthesized to yield edge map of the image. However for better edge vision the analyzed detail bands are appropriately thresholded before synthesis to avoid unwanted details. The LL band can be further decomposed by iterating the similar filter banks yielding second level decomposition and can be iterated further up to the permissible level giving nth level decomposition. This process is termed as pyramidal decomposition of the image. The image is decomposed in a hierarchy of resolutions, while considering more and more resolution layers, we get more and more detailed look at the image. The appeal of such an approach facilitates retention of structural contents that might go undetected at one resolution may be easy to spot at another which has been exploited for edge detection coupled with noise suppression.

### Conclusion

The wavelets could not be effectively used till Mallat discovered that continuous wavelet basis formed by inner products of orthonormal basis can be implemented by a band of constant Q filters, the non overlapping bandwidths of which differ by an octave. A lot of similarities have been found in FWT and subband coding. The highpass  $h_1[n]$  and lowpass  $h_0[n]$  used in figure 3.4 for subband coding have been used interchangeably as  $h_\psi[n]$  and  $h_\phi[n]$  respectively for clarity where

needed without the loss of generality in the wavelet implementation through filter banks.

62

## ***Chapter 4***

### **Novel Edge Detector**

#### **4 Introduction**

Different edge detectors in spatial domain, frequency domain and wavelet based operators have been explained in the previous chapters. These detectors differ in structure and characteristics. One of the major dilemmas in edge detection is the choice of optimum threshold which is not generic. There exists no set derivation or established procedure to find the optimal threshold, rather it is empirically established. It is assumed to be function of edges thickness, structure, characteristics of gradient operator and smoothing filter. On the other hand coarse scale operator is needed to determine coarse edges. Fine scale edge detector is suitable for detecting sharp intensity variations in the image.

Therefore multiscale approach is an excellent solution to obtain edges at different scales and then final edge map is obtained by combining them together.

Different detector may have explicit characteristics such as an operator may be good to determine straight edges like roads and rivers and may not be equally good to extract contours in an image. Therefore, it is intricate to find a general purpose edge detector which behaves well in all scenarios.

This chapter presents a novel edge detection paradigm in which innovative wavelet synthesis of detail bands based on bilinear interpolation and WSC is conceived such that the reconstructed image fabricates its edge map. The

63

proposed edge detector works over noisy images and claims to have better result in noisy environment. It works without user intervention for the choice of optimum thresholding. Since edge detection through WSC is a novel paradigm, the edge map obtained needs post processing optimizations such as hysteresis thresholding [16], non maximal suppression, edge thinning and linking.

#### **4.1 Edge Thinning**

Much work has been done on the thinning of "thick" binary images that are produced during edge detection, especially in proposed edge detector. Attempts have been made to reduce shape outlines which are many pixels thick to outlines which are only one pixel thick. Besides, noise in the images results in jaggy and discontinued edges and necessities edge enhancement in the form of edge linking or truncating noise pixels attached to the edges.

64

**Figure 4.1** Examples of the different thinning rules

65

algorithm.

## **4.2 Novel Wavelet Synthesis for Edge Detection**

Proposed method of edge detection is a novel paradigm in which image is being decomposed by wavelet analysis. An input image is decomposed using 2-dimensional discrete wavelet transform with decomposition limited to four levels. Each level of decomposition produces four images decimated by a factor of 2. Filter bank containing two filters (The wavelet function filter and scaling function filter) produces vertical, diagonal, horizontal and low pass residual details each stored in a decimated image. Low pass image is again fed to filter banks for next level of decomposition. Low pass image obtained at the fourth level of decomposition is then discarded. Figure 4.2 to figure 4.4 show decomposed images containing horizontal, vertical and diagonal details of three test images; Lina, House and Camera man. All the decomposed images are then adaptively thresholded using employing hysteresis in thresholding with threshold values based on statistical parameters. The wavelet coefficients obtained after thresholding are then interpolated.

66

**Figure 4.2** Lina Image decomposed in to four levels using DWT. H, V and D represent horizontal, vertical and diagonal respectively. Numbers show the level of decomposition.

**Figure 4.3** House Image decomposed in to four levels using DWT

67

**Figure 4.4** Camera man image decomposed in to four levels using DWT

Scale multiplication of wavelet coefficients is performed with view not only to capture details that may be detected on some other resolution but also to suppress noise. Resulting images containing horizontal, vertical and diagonal details are then fused together to obtain a edge map. Post processing is being performed for edge thinning, linking and truncating spurious details attached with edges. Detailed procedure is documented below and explained graphically in figure 4.5:-

S-1 Input image is converted to gray scale and size is ensured to be 512 x 512 pixels.

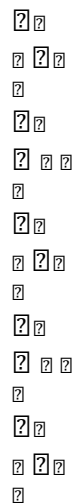
S-2 Using Daubechies wavelet, input image is filtered. Since image is a two dimensional signal, filtering will produce two 2-dimensional signals or four

68

images. As discussed in wavelet theory, the decomposed images will contain three images with high frequency details and one image containing low pass residue.

**Figure 4.5** Wavelet analysis filter banks and its synthesis for edge detection for  $n=4$ .  $A$ ,  $H$ ,  $V$  and  $D$  represent decimated approximations, average, horizontal, vertical and diagonal coefficients. Subscripts indicate decomposition level.  $\psi_1$ ,  $\psi_2$  and  $\psi_3$  represents horizontal, vertical and diagonal interpolated edge maps after point wise multiplication of concordant band coefficients up to 4th level.  $E$  is the resultant edge map of the image.

THRESHOLDING  
 $\mu + \sigma$   
 INTERPOLATION  
 EDGE ENHANCEMENT  
 IMAGE E



??

?? ? ?

?

??

?? ? ?

??

70

Figure 4.5 shows the practical implementation of proposed algorithm. The optimum decomposition level is not generic. Results were compiled up to fourth level wavelet decomposition based on subjective analysis. Figure 4.5 shows the wavelet analysis filter bank for the input image I followed by its synthesis filter bank for edge detection for n=4. E is the resultant image edge map. The analytical expression for WSC edge detection is as follows:

?? ? ? ? ?

?

?

???

### 4.1

?? ? ? ? ?

?

?

???

### 4.2

?? ? ? ? ?

?

?

???

### 4.3

? ? ? ? ?

?

???

### 4.4

? ? ?

??

? ? ? ? ? ?

?

?

???

?

???

?

??

### 4.5

71

Where  $\psi$  represents the synthesis of all the detail band coefficients by the

given technique, superscript  $d=1,2,3$  represents interpolated horizontal, vertical and diagonal detail bands to the original image size after multiplication of concordant bands, subscripts  $l$  represents the decomposition level.  $E$  is the resultant edge map of the image. The decomposition level  $n$  depends upon the image resolution, noise intensity/ model and its structural parameters which includes the edge thickness, length and statistical parameters.

### 4.3 Graphical User Interface for Software Development

Matlab has been used to develop software for the implementation both classical edge detectors and wavelet synthesis. Builtin matlab functions have been used to implement classical edge detection techniques. A Graphical User Interface (GUI) has been designed with a view to tune different parameters, such as noise type with control over mean and variance of the noise induced and choice of threshold (Default or manual). GUI contains an active X control to load images without the need of recompilation required with change in input image. While implementing edge detection through wavelet scale correlation, the GUI allows to choose various interpolation techniques and comparing the results. GUI also provides functionality to view the result of novel technique before and after edge enhancement. Snapshots of the GUI has been shown in Appendix B with necessary elaboration over various functions used.

### 4.4 Experimental Results

The edges detected by WSC compared with Canny edge detector for bench mark image are shown in figure 4.6.

72

$N(0, 0.01)$  Edges through WSC Edges through Canny

73

**Figure 4.6** WSC compared with Canny edge detector

The proposed edge detector has outperformed the classical edge detectors at default threshold. Canny failed to produce edge map of Lena at default threshold for Gaussian noise of variance .02 or above, whereas proposed scheme has given an adequate edge map of Lena with Gaussian noise of variance as high as 0.1 as shown in figure 4.7.

(a) (b) (c)

**Figure 4.7** Edge map obtained by WSC, with Gaussian Noise (a) 0.02, (b) 0.05 and (c) 0.1

Thick edges are vulnerable at multiple scales, thus are prominent in the final edge map detected by proposed algorithm. Edge enhancement is thus a requirement to enhance the edge map. Figure 4.8 shows the comparison of two images in which edge map obtained by WSC is shown before and after edge enhancement.

74

**Figure 4.8** Edge map obtained by WSC (Left) no edge enhancement (Right) Edge thinning followed by edge alignment.

Figure 4.8 shows Lena image edge map before and after edge enhancement. Using edge thinning, aligning and suppression of isolated pixels do produce sharp edges besides further denoising however, loss of edge pixels is clearly obvious during this process.

#### 4.4 Conclusion

75

#### 4.5 Future Work

- Establishing dependence of wavelet decomposition level on image resolution, statistical parameters, structure or type of image and noise level or model is open for future research.
- Optimal wavelet decomposition level for the image be worked out to determine optimal wavelet synthesis by scale correlation for edge detection.
- Edge enhancement remains a major task to improve / enhance the noisy edges.
- Edge cleaning or edge refinement techniques may be cascaded.

Lena  
Building

#### Benc

a  
g  
76

#### ch Mark I

Camera Ma

#### Images

n  
House  
Boat

#### Appendix A

77

#### Appendix B

### Snapshots of GUI for Software Development

**Figure B-1** GUI developed in Matlab: Left side is the control panel for various options required in edge detection. Right side shows edge detection results both on original and noisy images

78

**Figure B-2** Snapshot of Control Panel

Active X control to  
load the images  
Noise Distribution  
panel is used to  
incorporate random  
noise with adjustable



mean and variance

Threshold panel

allows to choose

both default and

manual thresholds

Wavelet Synthesis Panel

implements the novel

technique with control over

interpolation techniques

required during image

reconstruction.

Edge Enhancement

is performed over

reconstructed

image containing

final edge map

Edge Detector Panel

is use to compare

results of classical

operators